Royo Pastor, R.; Albertos Arranz, M.; Cárcel Cubas, JA.; Payá Herrero, J. (2012). Thermographic study of the preheating plugs in diesel engines. Applied Thermal Engineering. 37:412-419. doi:10.1016/j.applthermaleng.2011.11.059.

Thermographic study of the preheating plugs in diesel engines

R. Royo [a], M.A. Albertos-Arranz [b], J.A. Cárcel-Cubas [b], J. Payá [a,*]

[a] Instituto de Ingeniería Energética IIE, Universidad Politécnica de Valencia

Camino de Vera s/n, Edificio 8E cubo F planta 5, 46022 Valencia, Spain

[b] Renault Spain, Cta\ Madrid Km 185, 47008 Valladolid, Spain

Abstract

The use of direct injection diesel engines has been widely applied during the past ten years. In such engines, the preheating plugs are a key element which has a significant contribution in the pollutant emissions.

In this paper, two different plug designs from Renault are analyzed. The new plug reduces substantially the required electrical consumption. Nevertheless, the pollutant emissions are higher (fundamentally CO and HCs) and hereby a thorough analysis is required to understand the possible reasons.

Firstly, an infrared thermography analysis of the plugs has been carried out. The new plug tip presents 100-200ºC higher temperatures than with the former design. Secondly, a thermal model has been developed and validated with temperature measurements. The latter model has helped to obtain the energy flow diagram. Finally, a thermography analysis of the head of the cylinders has been carried out. The results show that the higher exhaust emissions are related with an incomplete combustion process due to a thin air gap which surrounds the tip of the plug.

Keywords: Diesel engines, preheating plugs, infrared thermography, thermal model

*Corresponding author. Tel.: +34 963879910; Fax: 34 963877272;

E-mail address: jorpaher@iie.upv.es (J. Payá)

NOMENCLATURE

J	Total radiation, W m^{-2}
E	Emitted radiation from the surrounding surfaces, W m^{-2}
σ	Stephan-Boltzmann constant, 5.67 x 10^{-8} W m^{-2} K^4
G	Reflected radiation from the surrounding surfaces, W m^{-2}
ε	Emissivity, adimensional (averaged value at the wavelength range of the camera detector: 8-14 microns)
T	Temperature, K
m	Mass, kg
c_p	Specific heat, J kg^{-1} K^{-1}
I	Intensity, A
V	Voltage, V
Q	Thermal power, W
Δt	Time step, s
C	Thermal capacitance, J K^{-1}
A	Heat transfer area surrounding the plug, m^2
h	Heat convection coefficient, W m^{-2} K^{-1}

Subscripts

conv	Convection
rad	Radiation
cond	Conduction
air	Air surrounding the plug
refl	Reflected radiation
old	Old preheating plug
new	New preheating plug

1. Introduction

In the past ten years, diesel engines have been widely used in the automotive industry in Europe [1] due to their higher efficiency, fuel economy and reliability.

Progressively, Direct Injection (DI) diesel engines have replaced the Indirect Injection engines. The main advantages are the reduction of the fuel consumption [2] and the favorable characteristic torque profile. Additionally, with the use of turbo-charging, a high performance is now achieved even for small and medium DI diesel engines, which now deliver specific brake powers close to those of spark ignition engines [3].

Nevertheless, the pollutant emissions are a key issue in the development of diesel engines given the recent restrictive legislations. Most of the pollutant emissions are produced during the engine start and warm-up [4-6], where the emissions of CO, HC and smoke are significant. These emissions are often caused by difficulties in obtaining a stable and efficient combustion under these conditions [3]. During the rest of the operation conditions from the engine, particularly for a constant charge and engine speed, the emissions are generally lower.

In order to start the operation of DI diesel engines, preheating plugs are mandatory to achieve the desired thermal conditions when the fuel is injected in the combustion chamber. Nevertheless, the preheating plugs require a considerably high electric energy consumption from the battery. Thus, the improvement of their design is a key issue to reduce both the energy consumption and the pollutant emissions.

In this paper, and for the first time, two different plugs of RENAULT have been characterized by means of infrared (IR) thermography. In comparison with other conventional measurement techniques such as with thermocouples or thermo-resistances, IR thermography presents the advantage of providing an instantaneous response to any temperature variations. Furthermore IR thermography is a non-intrusive tool [7] to characterize small elements such as the preheating plugs of a vehicle. Otherwise it would be hardly possible to measure the plug temperature under real operating conditions, as the insertion of thermocouples would modify the heat transfer conditions. Infrared (IR) thermography has already proved to be a useful technique in a wide variety of applications such as in the automotive sector [8-10], building inspections [11-12], HVAC installations [13-14] or in the characterization of heat exchangers [15-16].

2. Experimental set-up and methodology

2.1. Description of the preheating plugs

This paper analyzes the preheating system of a RENAULT Meganne III K9K engine. The main features of the engine are given in Table 1. The engine has a DI common rail with a turbo-compressor which has a displacement of 1.4 l. Fig. 1 shows a scheme of the preheating plug next to the cylinders where the combustion takes place. The tip of the plug is located inside the combustion chamber.

Two different plug designs have been analyzed. Figs. 2 and 3 show the detailed geometry of the tip of the old and new plug respectively.

The former preheating plug has a bigger diameter (4 mm) than the new plug (3.3 mm). Hence, the new plug has a bigger space between the plug and the cylinder head. This air gap or crevice can have a significant effect on the exhaust gas emissions [5] as discussed further on in the paper.

2.2. Analysis of the exhaust emissions

Before starting the engine, the combustion chamber and the fuel/air mixture are cold. In DI diesel engines, preheating plugs are required in order to increase the temperature rapidly and herewith ensure a complete combustion since the start-up.

Typically, the preheating plugs are used during the first 3 minutes (180s). Nevertheless, the vehicle industry has to guarantee an accurate performance of the plugs during a whole period of 300s.

Using a preheating plug implies a higher load for the engine, as it has to deliver the required power via the alternator. Thus, the plugs have two opposite effects: on the one hand, they can help decrease the pollutant emissions by improving the combustion process, but on the other hand, they increase the exhaust emissions because the engine has to deliver more power.

For these reasons, the pollutant emissions have been measured with internal and external feeding. In the first case, the power is directly provided to the plugs via the alternator, as in real conditions. In the second case, with external feeding, a battery feeds the plugs.

The exhaust gas emissions have been measured following the control standards 70/220/EEC, directive Euro 4. The pollutant emissions are measured in a test bench which simulates the New European Driving Cycle (NEDC).

2.3. Infrared thermography measurements

In the combustion chamber, many parallel chemical reactions take place. The formation of NO_x, CO and HC is directly correlated with the temperature [5]. Thus, the measurement of the temperature field around the plug provides complementary information to the exhaust emission tests.

The temperature of the plugs and the cylinder head have been measured by means of IR thermography for both the former design and for the new design. IR cameras enable the measurement of the surface temperature of opaque objects. The radiosity from opaque surfaces can be expressed as:

$$J = E + \rho \cdot G \tag{1}$$

Thus, the radiosity (output radiation) can be considered as the addition of the corresponding emission (E) and reflected irradiation (G) from the surrounding surfaces.

From the Stephan-Boltzmann Law for real (non-blackbody) surfaces, the emitted radiation (E) and the reflected irradiation (G) can be calculated as given in Eqs. (2) and (3) respectively.

$$E = \varepsilon \cdot \sigma \cdot T^4 \tag{2}$$

$$G = \sigma \cdot T_{refl}{}^4 \tag{3}$$

In the previous equations, T is the object temperature and T_{refl} is the apparent reflected temperature which is the object parameter of the infrared camera that takes into account the effect of the irradiation from the surrounding surfaces. It is also referred to as “Apparent temperature” since it is a temperature which is

related to the entire irradiation from the background independently from the possible sources.

The measurements of temperature with IR thermography are subject to uncertainties concerning the determination of the typical “Object parameters” (emissivity, reflected apparent temperature).

Table 2 shows the uncertainty of the temperature measurements. In the tests, a real temperature of the heating plug of 1000ºC and an apparent reflected temperature of 20ºC were obtained. An experimental test was carried out to measure the effective emissivity of the tip of the plug, and a value of 0.95 was found. As shown in Table 2, even for values of 0.96 or 0.94, the estimated temperature from the IR camera would only vary between +0.34% and -0.33%. Thus, there is a very small uncertainty due to the emissivity.

The uncertainty due to the apparent reflected temperature is even lower than for the emissivity. Even if the apparent reflected temperature were of 10ºC instead of 20ºC, the temperature estimated by the infrared camera would be 1000.006ºC.

The conclusion from this uncertainty analysis is that, for so high emissivities and temperatures, the effect of uncertainties in the estimated object parameters is almost negligible. Thus, the use of the IR camera is very appropriate for this application.

2.4. Thermal model of the plugs

In addition to the experimental tests, a thermal model has been developed in order to predict the plug temperature and quantify the heat dissipation towards the surroundings of the plug.

Given the small dimensions of the plug tip, a uniform temperature model (Eq. (4)) has been applied. The thermal power of the plug is dissipated via the following heat transfer mechanisms [17]:

- Convection heat transfer with the external air at 20ºC
- Radiation heat transfer to the surrounding walls
- Conduction towards the cylinder head

$$m \cdot c_p \cdot \frac{dT}{dt} = I \cdot V - A \cdot h \cdot (T - T_{air}) - A \cdot \varepsilon \cdot \sigma \cdot \left(T^4 - T_{refl}^4\right) - \dot{Q}_{cond} \qquad (4)$$

By introducing the thermal capacitance of the plug ($C = m.c_p$) and by applying a time-discretization to Eq. (4), the plug temperature T^{n+1} for any time step n+1 can be calculated directly as a function of the previous temperature (T^n) and as a balance of the heat transfer with the surroundings:

$$T^{n+1} = T^n + \frac{\Delta t}{C} \cdot \left[I^{n+1} \cdot V^{n+1} - A \cdot h \cdot (T^{n+1} - T_{air}) - A \cdot \varepsilon \cdot \sigma \cdot \left(T^4 - T_{refl}^4\right) - \dot{Q}_{cond} \right] \quad (5)$$

The results and parameters of the zero dimensional model represented in Eq. (5) are analyzed further on in subsection 3.3.

3. Results and discussion

3.1. Exhaust emissions

In the first measurement campaign with internal feeding, the CO_2 emissions were analyzed during the first 180s after the engine start. The new preheating plug decreased the CO_2 levels in around 20%.

In the second measurement campaign with external feeding, an increase of HCs of 5.9% and 3.4% of CO was detected with the new plug. Both pollutants are related with a deterioration of the combustion process and hereby, they require a specific analysis. As a first hypothesis, it seems that the differences in the exhaust emissions may be due to the crevice which surrounds the plug. It has been found [5] that narrow entrances in the combustion chamber often provoke a flame quenching, and consequently, the fuel/air mixture inside cannot be fully burnt. In order to support this hypothesis, the temperature of the plugs has been studied in detail by means of infrared thermography.

3.2. Temperature measurements of the tip of the plugs

A FLIR THERMACAM S65 long wave IR camera was used with close up lenses to enlarge the resolution of the images given the small dimensions of the preheating plug.

The infrared images were taken with a frequency of 50 images per second, and were directly saved at the hard disk as infrared radiometric sequences.

The cylinder temperatures were measured once steady-state conditions were achieved at the tip of the plug. Fig. 4 shows the thermography measurements of 4 cylinders in steady-state conditions. All of the images in Fig. 4 have been adjusted with the same temperature span and level.

In Fig. 5, the temperature evolution of the preheating plugs is represented. In comparison with the old plug, the new plug induces clearly higher temperatures in the cylinders.

By analyzing Figs. 4 and 5, the following results are obtained:

- The new plug shows quite uniform and averaged steady temperatures around 1000ºC
- The temperature variations with the old plug are higher, with tip temperatures varying between 780ºC and 930ºC.
- It seems that the pollutant emissions of the new design are not related with the temperatures at the tip of the heating plug, since the newly designed plug presents higher and more uniform temperatures and less variations between cylinders than with the previous design.

A deep and detailed thermal study of the tip of the preheating plug and the surface of the cylinder head is hereby necessary to explain why the exhaust emissions are higher with the new plug. The model results given in section 3.3 provide interesting information which help understand the infrared thermography results of the head of the cylinders (section 3.4).

3.3. Model results

Before analyzing the model results, it is first essential to consider the different schedules of the electric power supply of each plug. As explained previously, the new plug is designed to save electrical energy. This aspect is clearly shown in Fig. 6, where the heating power of both plugs is represented.

In total, during the 300 s represented in Fig. 6, the new plug requires 69% less energy consumption than the former plug. This aspect is very attractive given the fact that the electric consumption of the auxiliaries is continuously increasing in vehicles.

Fig. 7 shows the experimental and calculated temperature profiles by means of Eq. (5). The experimental test in Fig. 7 can be divided into three phases:

- Initial transient heating of the plug
- Steady-state heat transfer region
- Final cooling of the plug

Although some minor differences are detected in the initial transient heating process, the prediction of the steady-state performance and of the final cooling process is very accurate (±2%), hereby supporting the use of the uniform temperature model.

Fig. 8 shows the final transient cooling of the plug which is of particular relevance in the calculation of the thermal capacitance of the plugs.

The thermal capacitance of the plugs ($C = m.c_p$) has been obtained by means of the temperature profiles during the final transient cooling process (last 10s in Fig. 8). The thermal capacitance has been calculated using the Excel Solver by minimizing the mean square error between the model and the experimental results shown in Fig. 7. The capacitance is important as it determines the velocity of the heating process, or equivalently, the necessary time to achieve a steady-state condition heat transfer.

For the former plug, a thermal capacitance of 20 J/K was found. For the fast plug, the best results are obtained for a thermal capacitance of 25 J/K. These results are coherent with the real physical parameters of both plugs. For instance, the former plug has a mass of 23 g and an estimated specific heat c_p of 900 J/kg K. This gives a thermal capacitance of 20.7 J/K which is very close to the value 20 J/kg found with the uniform temperature model.

The fast plug has a mass of 26 g, and the same specific heat as the former one. Thus, a thermal capacitance of 23.5 J/K is obtained, which is also in good agreement with the value of 25 J/kg which is found with the uniform temperature model.

Heat dissipation mechanisms

By means of the developed model, the different heat dissipation mechanisms have been quantified and they are summarized in Figs. 9 to 11. The values which are shown have been calculated at steady-state conditions. The parameters of the uniform temperature model are detailed in Table 3. The following results have been obtained:

- As inferred from Fig. 9, the new plug design induces higher temperatures in both the tip of the plug and in the crevice surrounding the plug.

- In the new plug (Fig. 10), due to the high temperatures which are achieved, radiation is the predominant heat transfer mode. From the generated 33 W, almost all of the power (28.3 W) is provided to the the combustion chamber.

- With the former plug (Fig. 11), from the entire 110W electric power provided at steady-state conditions, 92 W are directly conducted to the cylinder head, and indirectly to the combustion chamber due to heat conduction in the cylinder head. In total after 300s, as there are 4 plugs, 115000 J are provided to the cylinder head. 15.1 W are dissipated in the incandescent tip via radiation.

- In the old plug, assuming a cylinder head mass of 12 kg and a specific heat capacity c_p = 900 J kg^{-1} K^{-1}, this implies that from the heating induced by the conduction losses, a mean temperature increase of the cylinder head of around 10.6ºC is achieved. This temperature increase has been confirmed experimentally, as shown in the following section 3.4.

3.4. Results and analysis of the cylinder head temperature

From the infrared sequences obtained during the experimental characterization of both preheating plugs, it is also possible to analyze the temperatures of the surface of the cylinder head during the complete duration of the tests (300s). In this case, the temperature range used at the camera must be the lowest one (-40-160ºC). If the sequences are not registered in the adequate range, it is not possible to obtain correct temperature measurements.

In the next paragraphs, the results are analyzed for cylinder 1. Very similar results have been obtained for the other 3 cylinders. With the new design, high temperatures (150ºC) are found at the zone which surrounds the plug crevice.

Fig. 12 shows the temperature profile which is obtained in the cylinder head for different distances from the central plug axis. With the new design, the region near the axis reaches 150ºC, whereas the old plug presents temperatures below 100ºC. These differences in the plug crevice are reasonable given the fact that the new plug reaches higher temperatures at the tip of the plug.

The key point in this study is nevertheless the temperature which is achieved at the rest of the cylinder head. The materials which are used at the cylinder heads are aluminium alloys, which have high thermal conductivities and

diffusivities. Thus, the temperatures in the entire cylinder head are rather uniform. With the exception of the region right next to the plug (less than 5 mm in Fig. 12), due to the heat conduction, the old plug design induces approximately 10ºC higher temperatures in the cylinder head. This aspect is in coherence with the results of the uniform temperature model.

Figs. 13 and 14 show the temperature profiles which are obtained in the cylinder heads after 300s. After this time, the main part of the cylinder head surface where the old plug is mounted shows temperatures about 40ºC due to the residual heating of the entire cylinder head caused by the heat conduction.

On the right-hand side of Figs. 13 and 14, the isotherm camera tool has been used to represent in green the temperature range between 40ºC and 160ºC. As may be inferred from Fig. 13, a very large proportion of surface around the cylinder head has temperatures above 40ºC. On the contrary, in Fig. 14, where the results are given for the new plug, there is only a thin area in the crevice with such temperatures, and the rest of the cylinder head is colder than 40ºC.

4. Conclusion

In this work, a thermographic study of two different preheating plugs of a RENAULT diesel engine has been carried out. The temperature of the tip of the plugs and of the head of the cylinders has been measured. A uniform temperature model has been developed and has provided a very good agreement with the measurements. The model has provided a useful tool to quantify the heat transfer losses and to compare both plug designs. The following conclusions have been drawn:

- With the new plug design, almost the entire heating power is transmitted directly towards the combustion chamber as radiation. The new plug presents higher temperatures in the plug tip and in the plug crevice, but not in the rest of the cylinder head.
- With the old plug, less heating power is directly supplied to the fuel/air mixture via radiation, but due to heat conduction, the temperatures in the entire cylinder head are around 10ºC higher.
- The plug crevice is bigger with the new plug and thus, a bigger proportion of the fuel/air mixture is partially unburnt. This is the reason for the higher pollutant emissions which are observed with the new plug.

In conclusion, although the new plug reduces the electric energy consumption, the old plug is preferable because the temperatures are more uniform in the cylinder head, and the plug crevice is smaller, hereby reducing the exhaust gas emissions.

Acknowledgements

The authors gratefully acknowledge RENAULT SPAIN and RENAULT FRANCE for the funding of research projects during the past 20 years.

Bibliography

[1] Monoghan, M.L., Future gasoline and diesel engine review. Int. J. Automot. Techn. 1 (1) (2000) 1-8.

[2] Comité des Constructeurs Français d'Automobiles (2007), web site: http://www.ccfa.fr

[3] Broatch, A., Luján, J.M., Ruiz, S., Olmeda, P., Measurement of hydrocarbon and carbon monoxide emissions during the starting of automotive di diesel engines, Int. J. Automot. Techn. 9 (2) (2008) 129-140.

[4] Merkisz, J., Bielaczyc, P., Pielecha, J., Cold start emissions performance from direct injection Diesel engine, EAEC European Automotive Congress, Bratislava (2001).

[5] Heywood, J.B., Internal Combustion Engine Fundamentals (1988), McGraw-Hill, New York.

[6] Kim, H., Yoon, S., Lai, M.C., Study of correlation between wetted fuel footprints on combustion chamber walls and UBHC in engine start processes, Int. J. Automot. Techn. 6 (5) (2005) 437-444.

[7] Hung, Y.Y., Chen, Y.S., Ng, S.P., Liu, L., Huang, Y.H., Luk, B.L. Ip, R.W.L., Wu, C.M.L., Chung, P. S., Mater. Sci. Eng., R., 64 (5-6) (2009) 73-112.

[8] Carvajal, E., Jiménez-Espadafor, F. J., Becerra, J.A., Torres, M., Methodology for the estimation of cylinder inner surface temperature in an air-cooled engine, Appl. Therm. Eng. (31) (8-9) (2011) 1474-1481.

[9] Royo, R., Characterization of Automotion Brake Thermal Conditions by the Use of Infrared Thermography, Infrared Training Center and FLIR Systems (2004) 259-266.

[10] Royo, R., Characterization of the Exhaust Flow in the Catalytic Converter of a Spark Ignition Engine using Infrared Thermography, The Infrared Training Center (2003) 193-200.

[11] Balaras, C.A., Argiriou, A.A., Infrared thermography for building diagnostics, Energ. Buildings (34) (2) (2002) 171-183.

[12] Royo, R., Design of a Infrarred Inspection Maintenance Planning for Comercial Buildings, IEECB - Improving Energy Efficiency in Commercial Buildings (2004) 123-126.

[13] Rahman Al-Kassir, A., Fernandez, J., Tinaut, F.V., Castro, F., Thermographic study of energetic installations, Appl. Therm. Eng. (25) (2-3) (2005) 183-190.

[14] Royo, R., Torrella, E., Martín, A., Operating Cycle Analyses of Different Refrigeration Systems Using Infrared Thermography, Infrared Training Center and FLIR Systems (2005) 103-113.

[15] Ge, Z., Du, X., Yang, L., Yang, Y., Li, Y., Jin, Y., Performance monitoring of direct air-cooled power generating unit with infrared thermography, Appl. Therm. Eng. (31) (4) (2011) 418-424.

[16] Hemadri, V. A., Gupta, A., Khandekar, S., Thermal radiators with embedded pulsating heat pipes: Infra-red thermography and simulations, Appl. Therm. Eng. (31) (6-7) (2011) 1332-1346.

[17] Incropera, F.P., Dewitt, D.P., Bergman, T.L., Lavine, A.S., Fundamentals of Heat and Mass Transfer (2007) John Wiley & Sons

Table 1

Characteristic	Value
Fuel	Diesel
Bore (mm)	76
Stroke (mm)	80.5
Number of cylinders	4
Injection system	Direct injection common rail with turbo-compressor

Table 1. Engine characteristics of the RENAULT Meganne III K9K

Table 2

	Variable	Object temperature (ºC)	Variation (%)
Emissivity	0.96	996.7	-0.33
Reference: ε = 0.95	0.95	1000	0
	0.94	1003.4	+0.34
Apparent reflected temperature	10 ºC	1000.006	+0.0006
Reference T_{refl} = 20 ºC	20 ºC	1000	0

Table 2. Uncertainty of the temperature measurements

Table 3

Parameter	Old plug	New plug
Δt [s]	0.02	0.02
C [J/K]	20	25
A [mm^2]	134.5	197.5
Q_{cond} [W]	92	0
h_{conv} [$W\ m^{-2}\ K^{-1}$]	24	24
T_{air} [K]	290	290
ε [-]	0.95	0.95
T_{refl} [K]	290	290

Table 3. Parameters of the 0-D model

Figure 1

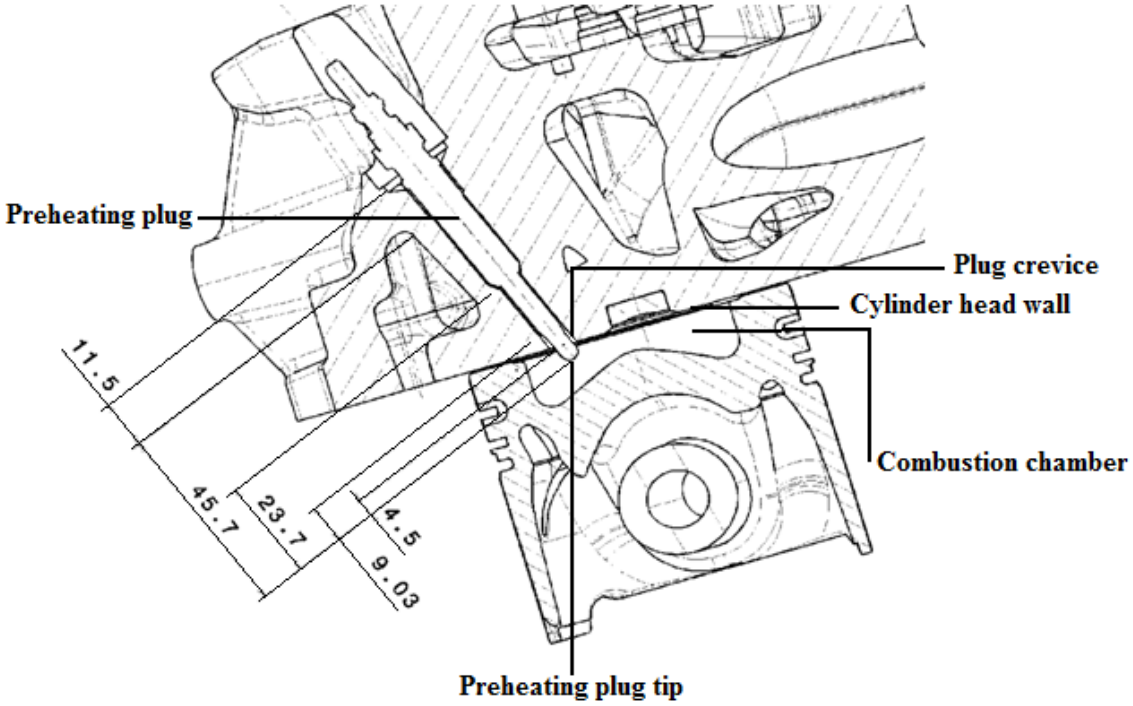

Fig. 1. General layout of the old preheating plug (units: mm)

Figure 2

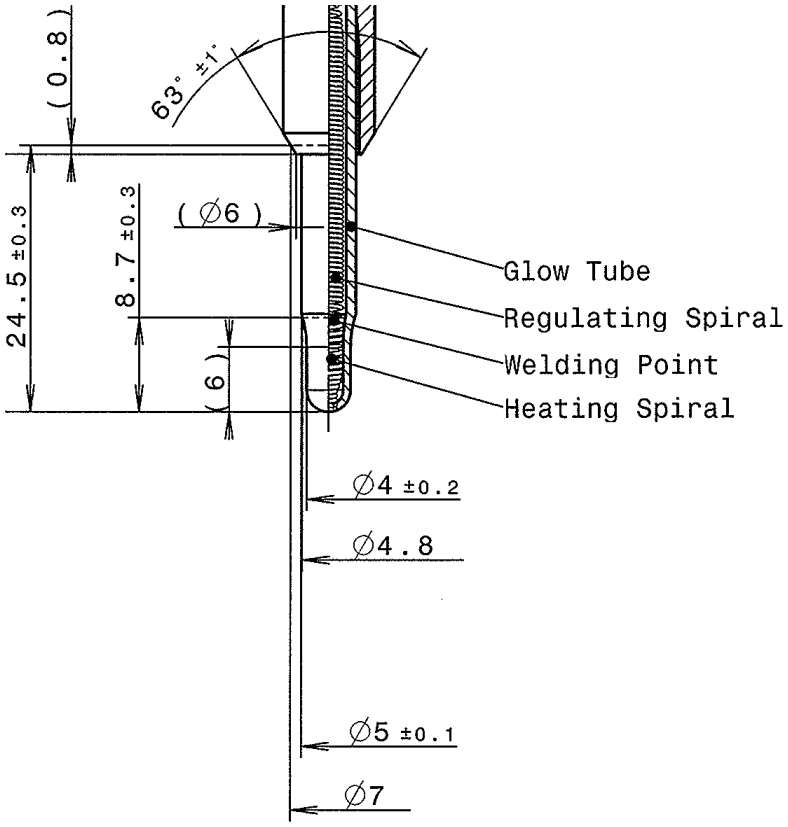

Fig. 2. Detailed geometry of the tip of the old plug (units: mm)

Figure 3

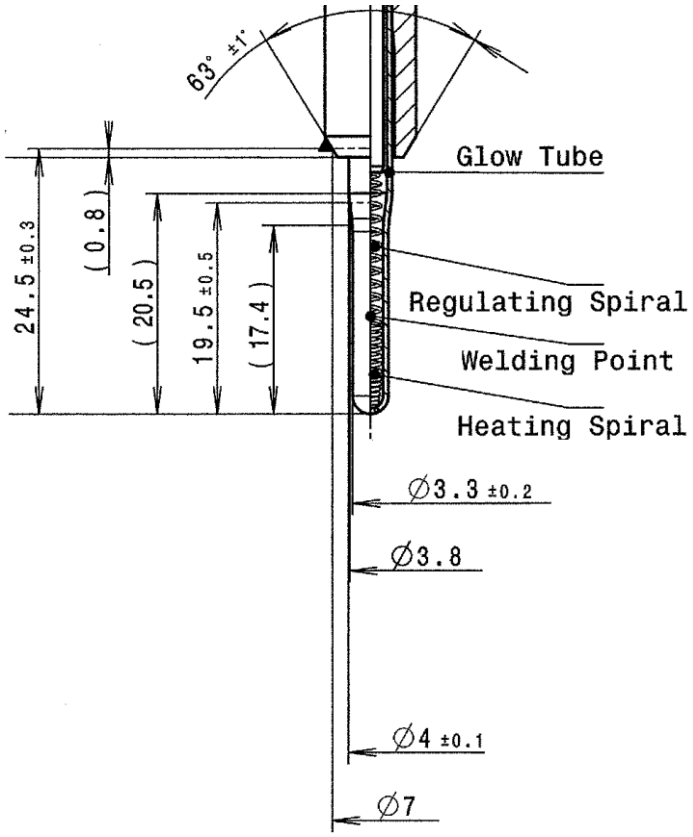

Fig. 3. Detailed geometry of the tip of the new plug (units: mm)

Figure 4

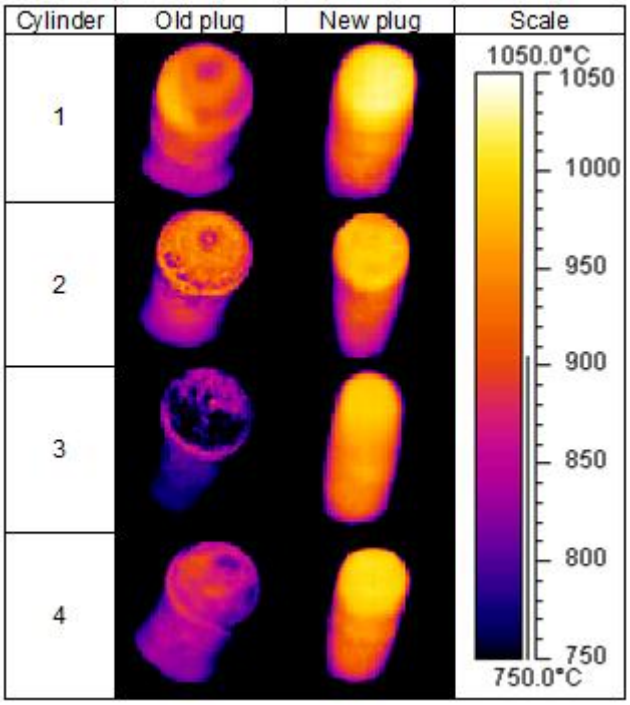

Fig. 4. Thermography of the cylinders

Figure 5

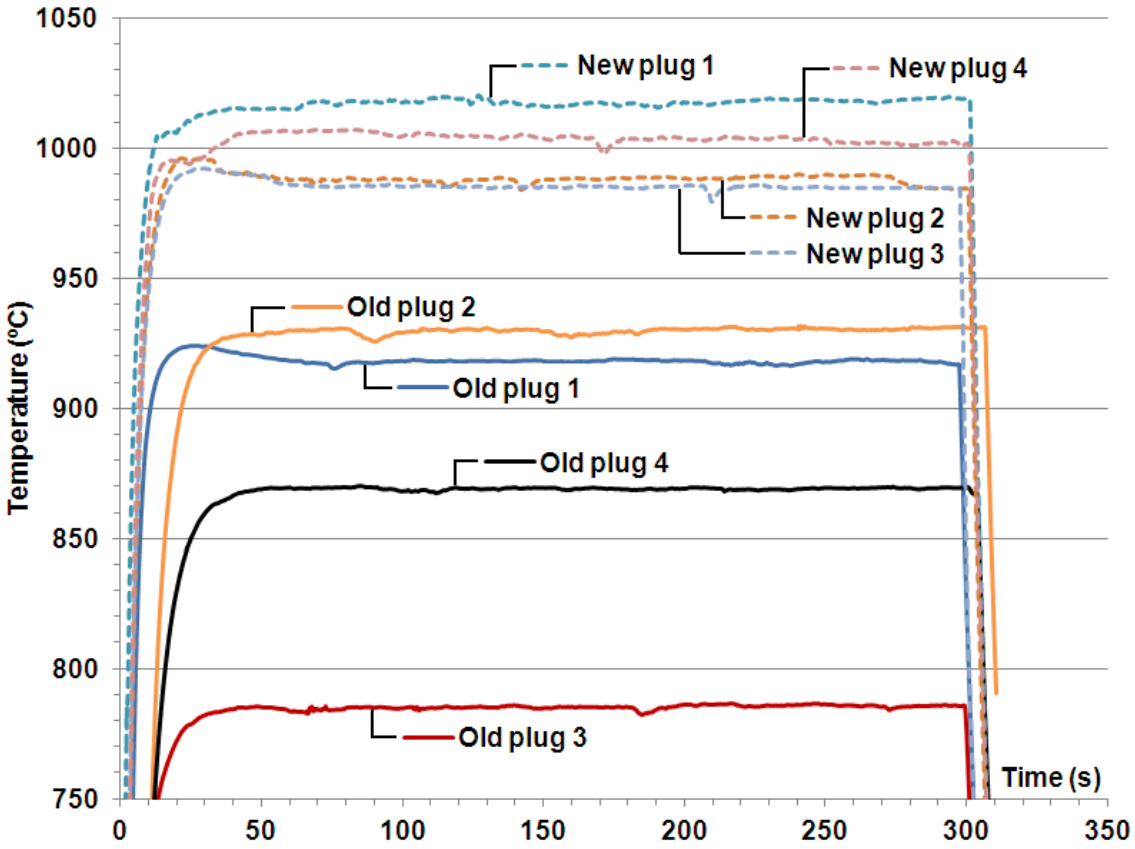

Fig. 5. Temperature evolution of cylinders 1 to 4

Figure 6

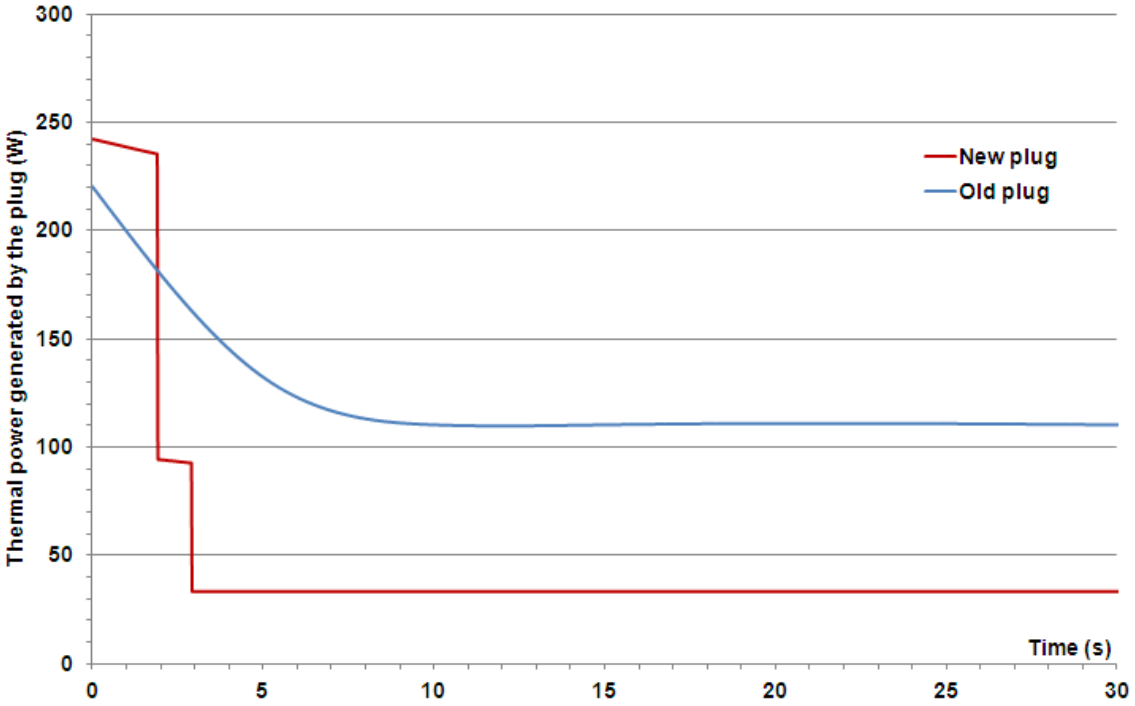

Fig. 6. Heating power of the plugs (from I.V measurements)

Figure 7

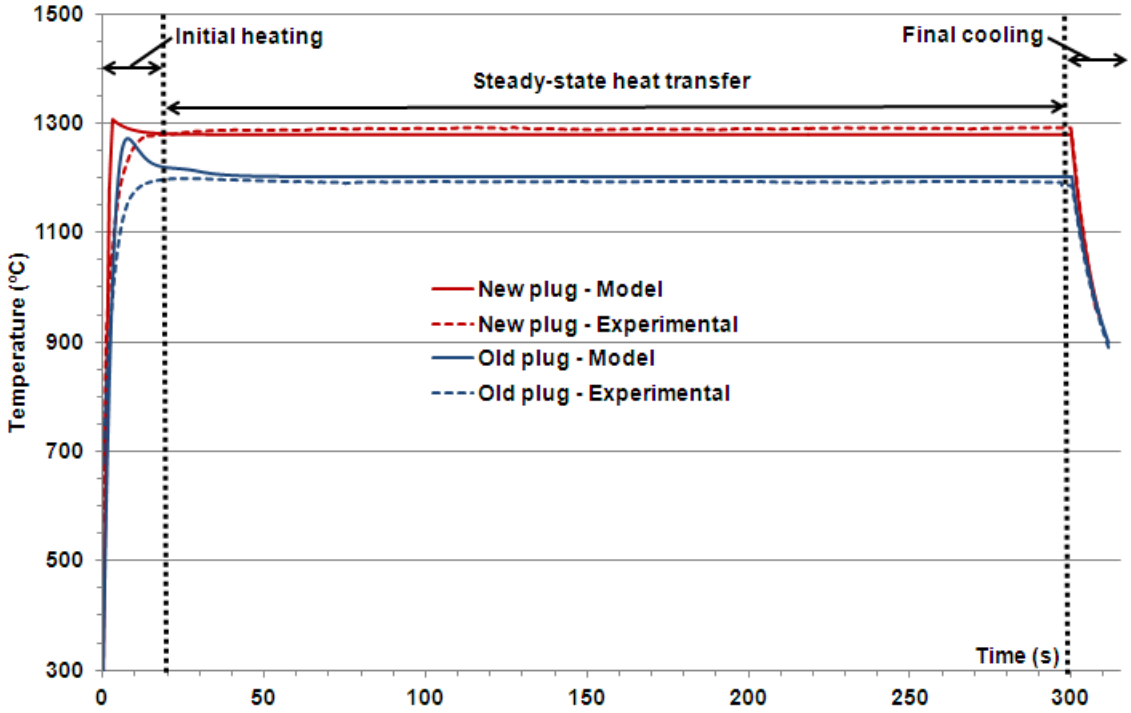

Fig. 7. Validation of the uniform temperature model in the complete test

Figure 8

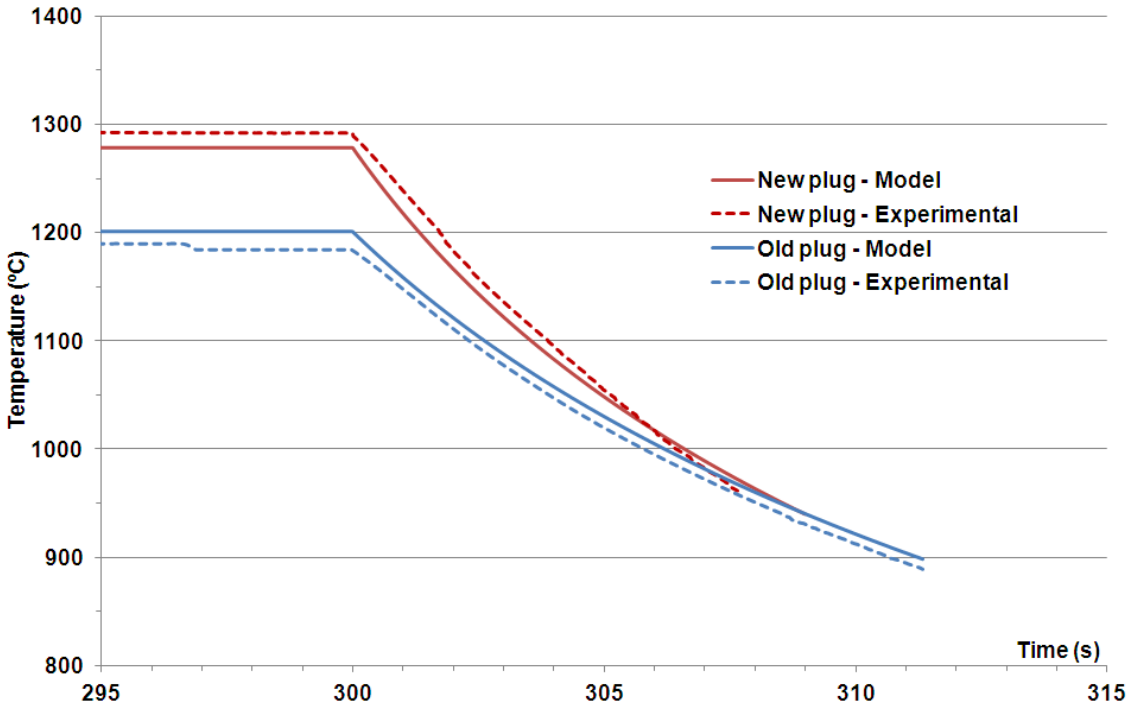

Fig. 8. Validation of the uniform temperature model in the final cooling process

Figure 9

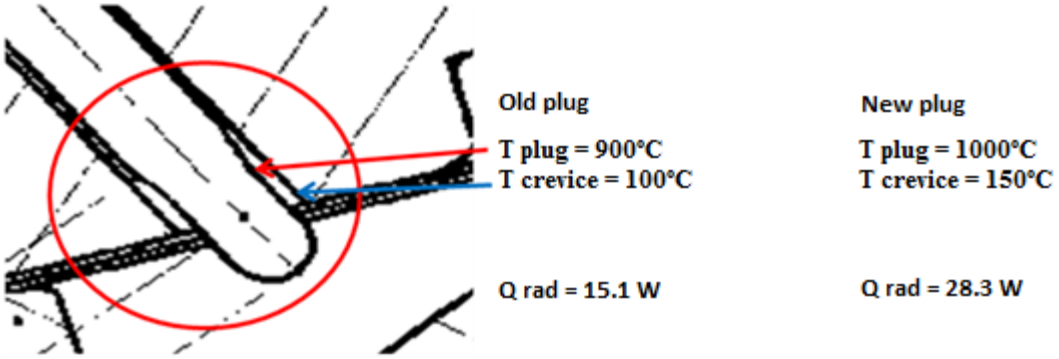

Fig. 9. Temperatures around the tip of the plug

Figure 10

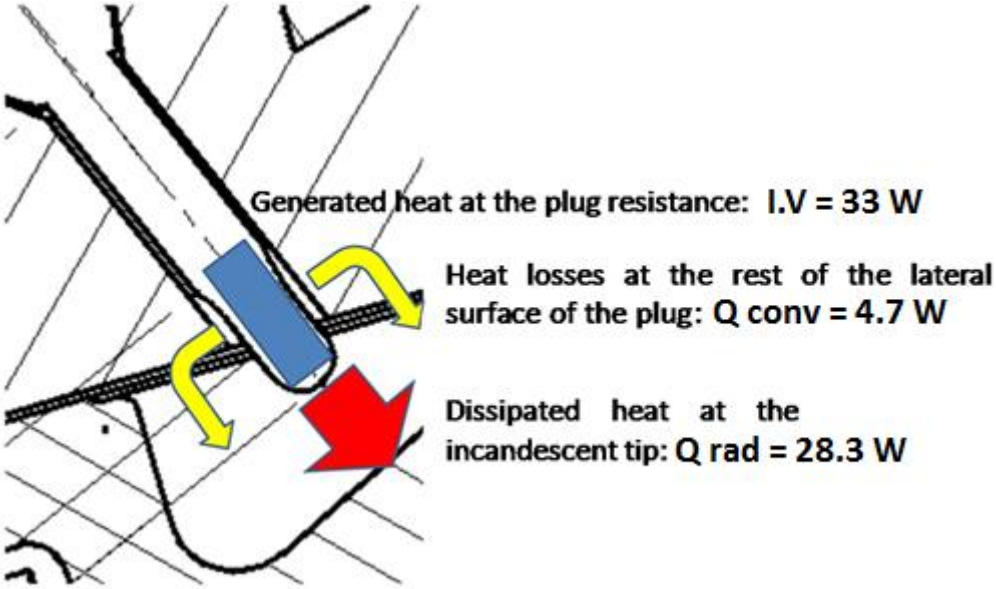

Fig. 10. Energy flow diagram for the new plug

Figure 11

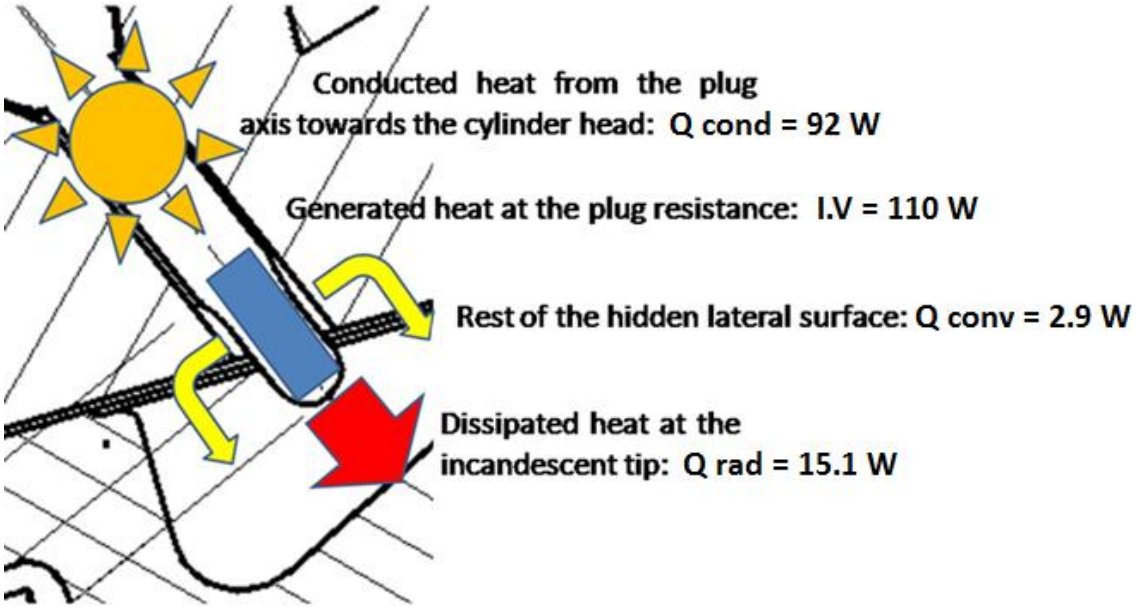

Fig. 11. Energy flow diagram for the old plug

Figure 12

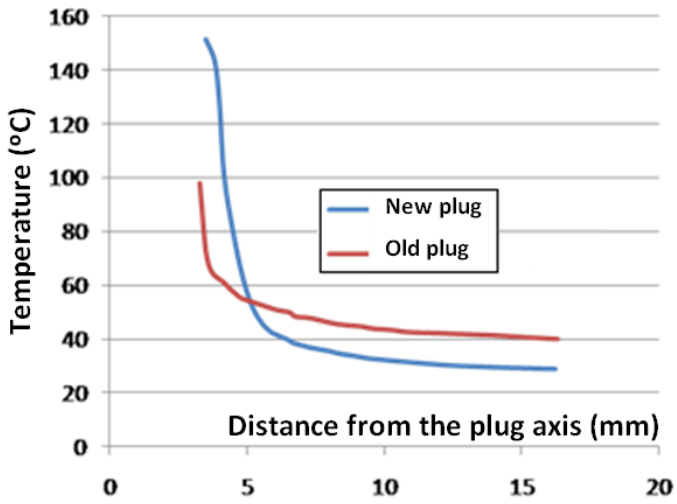

Fig. 12. Temperature near the cylinder 1 head surface after 300s

Figure 13

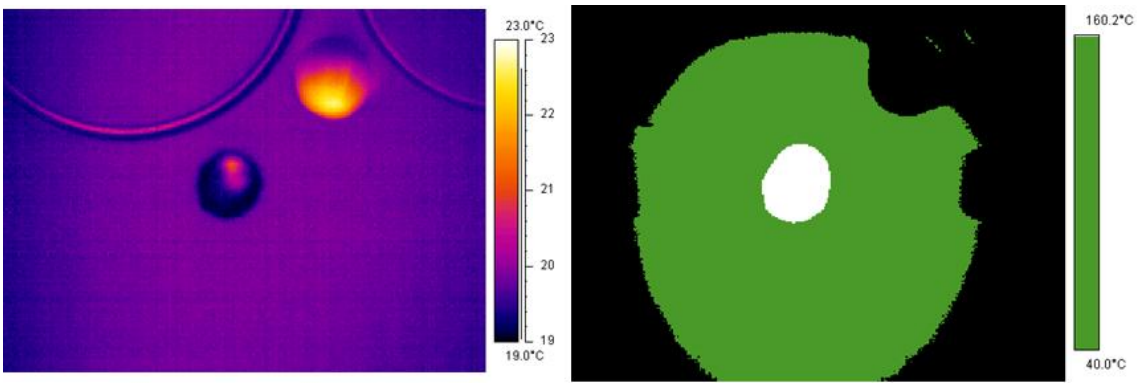

Fig. 13. Cylinder 1 head temperatures obtained with the old plug

Figure 14

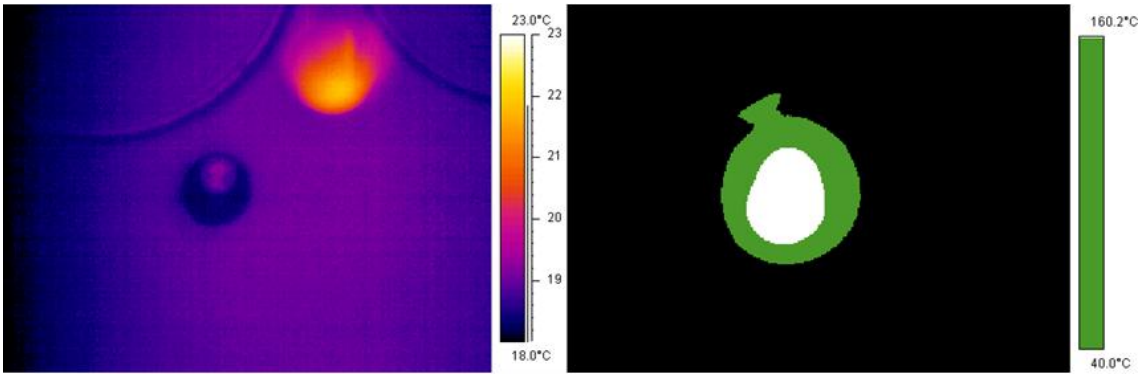

Fig. 14. Cylinder 1 head temperatures obtained with the new plug